Study on contact distortion during high aspect ratio contact SiO_2 etching

Jong Kyu Kim, Sung Ho Lee, Sung Il Cho, and Geun Young Yeom

Citation: Journal of Vacuum Science & Technology A: Vacuum, Surfaces, and Films **33**, 021303 (2015);
View online: https://doi.org/10.1116/1.4901872
View Table of Contents: http://avs.scitation.org/toc/jva/33/2
Published by the American Vacuum Society

Study on contact distortion during high aspect ratio contact SiO_2 etching

Jong Kyu Kim
Department of Advanced Materials Science and Engineering, Sungkyunkwan University, Suwon, Gyeonggi-do 440-746, South Korea and Memory Division Semiconductor Business, Samsung Electronics, San No. 16 Banwol-Ri, Taean-Eup, Hwasung-City, Gyeonggi-Do 449-711, South Korea

Sung Ho Lee and Sung Il Cho
Memory Division Semiconductor Business, Samsung Electronics, San No. 16 Banwol-Ri, Taean-Eup, Hwasung-City, Gyeonggi-Do 449-711, South Korea

Geun Young Yeom[a)]
Department of Advanced Materials Science and Engineering, Sungkyunkwan University, Suwon, Gyeonggi-do 440-746, South Korea

(Received 22 June 2014; accepted 27 October 2014; published 3 December 2014)

As pattern density is increased in semiconductor integrated circuits (ICs) and pattern sizes are decreased to nanometer scale, high aspect ratio contact etching has become one of the most difficult processes in nanoscale IC fabrication. The increase in aspect ratio of the contact oxide etching raises problems such as low mask selectivity, microloading, pattern degradation, and etch stops. In this study, the authors investigated the effect of various oxide etch conditions such as mask materials, mask thickness, and oxide etch processes, on contact profile degradation. The results showed that greater contact pattern distortion occurred as the aspect ratio of the etched oxide was increased. The use of amorphous carbon instead of amorphous silicon as the etch mask, and the use of a more carbon-rich gas composition, lessened pattern distortion. The polymer deposited at the interface between the mask layer and the oxide layer appeared to significantly affect the degree of contact pattern distortion. By adding an *in-situ* polymer removal step during the overetch of a multistep contact oxide etch process with a 20:1 aspect ratio, about a 7% improvement in pattern distortion could be obtained without changing other conditions. © *2014 American Vacuum Society*.
[http://dx.doi.org/10.1116/1.4901872]

I. INTRODUCTION

The pitch and pattern sizes of semiconductor circuits are being further and further miniaturized to achieve greater integration in semiconductor devices.[1] However, to maintain sufficient electrical conductivity, the conducting materials used for the electrical wiring need to be replaced by less resistive materials. Alternatively, the height of the patterns needs to be increased.[2] Increasing contact pattern height increases the thickness of the dielectric material separating the conducting material layers, thereby increasing the aspect ratio of the contact hole.

The increase in contact aspect ratio raises some significant problems during contact oxide etching. Namely, to etch a thick contact oxide layer without eroding the mask layer completely, a thicker mask layer is needed. Higher mask etch selectivity also is required, as the 3D etch effect accelerates mask etching for small pattern sizes, and a high ion bombardment energy is required during the contact oxide etching to maintain a vertical etch profile.[3] To improve the mask etch selectivity for high aspect ratio contacts (HARCs), researchers have investigated harder mask materials[4] or more selective etch chemistry.[5] Other major issues arise from the small contact width and deep contact depth. Decreased etchant delivery in the contact hole leads to microloading, and the enhanced polymer deposition in the contact hole causes an etch stop.[6] To overcome the problems related to microloading and the etch stop, process developments such as increasing the ion bombardment energy and the processes decreasing/controlling the polymer precursors during contact etching have been investigated.[7]

Recently, due to the increased aspect ratio of HARCs, contact pattern deformations such as contact hole tilting and contact hole distortion have also become critical issues during HARC etching.[8] Contact oxide tilting is the deviation of a contact hole's center to one side caused by increasing the etch depth. Contact oxide distortion is the change of a contact hole's shape to an irregular one different from the mask pattern shape, though the center of the contact oxide hole remains stable. Figures 1(a) and 1(b) show the scanning electron microscope (SEM) images for typical HARC pattern examples (aspect ratio of 13:1) of oxide hole tilting and oxide hole distortion, respectively. As shown in Fig. 1(a), for the contact hole tilting example, the distances between oxide hole centers were different (distance A $\neq$ distance B) due to the deviation of contact oxide hole centers. In the cases of contact hole distortion, as shown in Figs. 1(b) and 1(c), the distances between the oxide hole centers are the same (as shown with the layout matrix lines), but the shapes of the contact holes are not circular. The contact hole distortion decreases the overlay area of the contact hole with the lower layer, and therefore, contact resistance is increased. Similar to contact hole tilting, contact hole distortion is known to be caused by the asymmetric charging of the contact hole sidewall, which changes the local electric field in the contact

[a)]Author to whom correspondence should be addressed; electronic mail: gyyeom@skku.edu

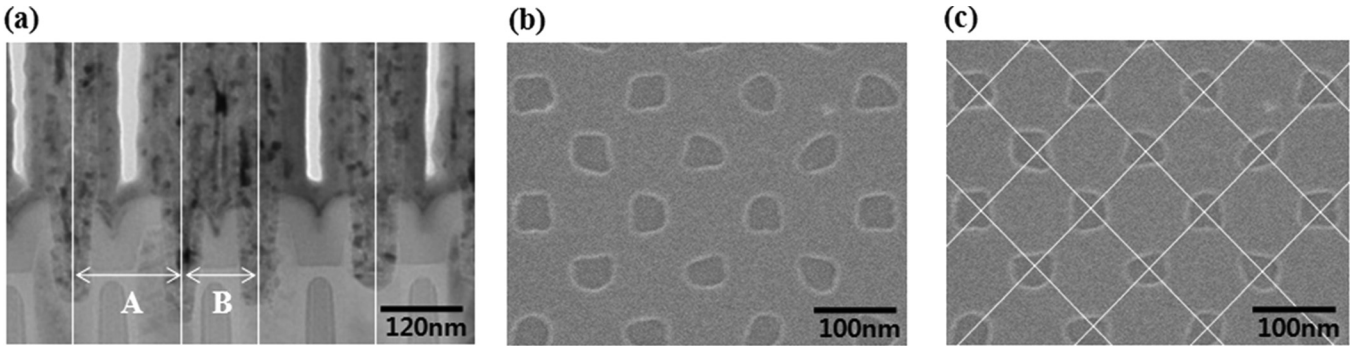

FIG. 1. Typical HARC pattern showing contact oxide hole tilting and contact oxide hole distortion for the HARC with an aspect ratio of 13. (a) Typical contact hole profile with tilting phenomenon (A ≠ B) observed by vertical SEM. (b) Typical phenomenon of contact hole distortion and (c) with layout matrix lines observed by top–down SEM.

hole and alters the direction of the reactive ions in the contact hole.[9]

Pulsed plasmas have been investigated as a way to alleviate contact-hole charging by removing the electron shading effect.[10] In addition, to decrease the amount of a nonuniform C-F based polymer layer that is deposited on the sidewall of the contact hole during the HARC etching process, the characteristics of C-F based gas dissociation have been investigated by experimentation and simulation.[11,12] However, the mechanism of contact hole distortion during HARC etching has not fully been investigated.

In this study, we investigated the variations in contact hole shapes as a function of increasing aspect ratio of the contact holes by varying the mask materials, etch gas chemistry, and other factors. The degree of contact hole distortion also was studied to understand the important factors affecting contact pattern distortion. Based on our results, we suggest an effective method for mitigating the contact hole distortion.

II. EXPERIMENTAL METHODS

The HARC oxide samples used in the experiment were made by sequentially depositing 500 Å of SiN, 16 000 Å of tetraethyl orthosilicate for the formation of HARC oxide, and 5000 Å of amorphous silicon layer as the mask layer on p-type silicon wafer. The amorphous silicon mask layer was patterned by depositing 2000 Å layer of SiO_2 and 60 Å of SiON as a multilayer mask, and by photoresist patterning of 80-nm contact holes using a 193-nm ArF immersion lithography tool (ASML). As a comparison to the amorphous silicon mask layer, 5000 Å of amorphous carbon also was deposited as the mask layer.

The amorphous silicon mask layer and the amorphous carbon layer were etched using a 300-mm inductively coupled plasma etcher (LAM Research Inc., FLEX 3X), and the oxide layers were etched using a capacitively coupled plasma etcher (Tokyo Electron Co. Ltd., VIGUS instrument).

HARC etching was carried out using a gas mixture composed of $C_4F_8/C_4F_6/O_2/Ar$ at 10 mTorr of pressure, $1500W_s$ of source power, $4800W_b$ of bias power, and the substrate temperature was 300 °K. The HARC layer was also etched using a multistep HARC etching method composed of a main etch process and overetch processes. In the multistep HARC etch process, the oxide was etched using a main etch recipe based on $C_4F_8/O_2/Ar$ just until the contact oxide was etched, and to increase the etch selectivity over the exposed contact silicon, overetch processes were conducted with mixtures of $C_4F_8/O_2/Ar$ and $C_4F_6/O_2/Ar$.

The contact etch profiles were observed vertically by using a SEM. The polymer layer deposited in the contact hole sidewall was observed using a transmission electron microscope (TEM). The contact hole distortion was observed by top–down SEM. To estimate the degree of contact hole pattern distortion, the contact hole oxide was partially removed from the top of the contact layer by layer using chemical mechanical polishing (CMP) and by observing the shape change of the contact hole remaining in the contact. The ellipticity of the contact hole was estimated by (the short contact hole width/the long contact hole width) × 100%; therefore, the ellipticity of the complete circular shape was defined as 100%.

III. RESULTS AND DISCUSSION

After the HARC etching of a contact hole with an aspect ratio of 16, the degree of contact hole distortion as a function of contact etch depth was observed by milling the contact holes gradually using a CMP method. Figure 2 shows the

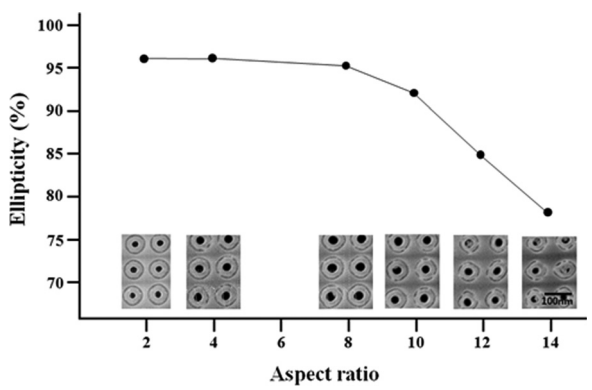

FIG. 2. Degree of contact hole distortion measured as a function of the aspect ratio of HARC with amorphous silicon mask. The HARC etching was carried out using a gas mixture composed of $C_4F_8/C_4F_6/O_2/Ar$, 10 mTorr, $1500W_s$ of source power, $4800W_b$ of bias power, and 300 °K of substrate temperature.

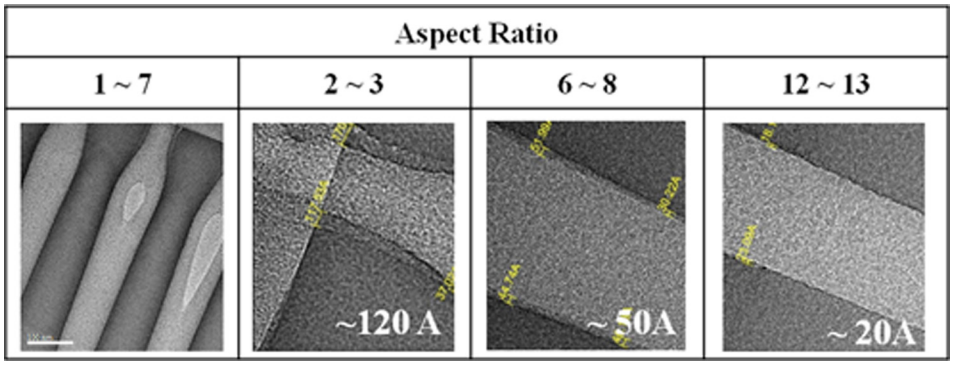

FIG. 3. (Color online) Thickness of C-F based polymer deposited on the sidewall of the HARC measured as a function of aspect ratio of a contact hole. The HARC etch condition was the same as that in Fig. 2.

shapes and calculated ellipticities of a contact hole with increasing aspect ratio (aspect ratio = the depth of contact hole/the width of contact hole). As shown, when the aspect ratio was low, the contact hole was barely distorted, but as the aspect ratio was increased, more contact hole distortion was observed, the ellipticity decreasing from about 96% for an aspect ratio of 2 to about 78% for an aspect ratio of 14. In this experiment, no significant contact tilting was observed.

The thickness of the C-F based polymer layer formed on the sidewall of the contact hole during the HARC etching was observed by cross-sectional TEM and the results are shown in Fig. 3 as a function of aspect ratio of the contact hole. The HARC etch conditions were the same as those in Fig. 2. As shown, the thickness of the polymer layer deposited on the sidewall of the contact was as thick as 117–170 Å when the aspect ratio was 2–3. As the aspect ratio was increased, the thickness of the polymer layer decreased and, at the aspect ratio of about 12–13, the thickness of the polymer layer was about 18–23 Å. This indicates that the increased distortion of the contact hole with increasing the aspect ratio was not directly related to the thickness of the polymer layer, as the polymer layer was thinner for the higher aspect ratio. However, as shown in the figure, the thickness of the polymer layer deposited on the sidewall of the contact was not uniform at a given aspect ratio value. Therefore, though we do not have conclusive evidence, our results suggest that thickness differences in the polymer layer on the contact sidewall may be partially related to the contact hole distortion.

To study other parameters affecting contact distortion during HARC etching, mask materials were varied from an amorphous silicon layer to an amorphous carbon layer. The effect of mask materials on the contact hole distortion was investigated and the results are shown in Fig. 4 for aspect ratios of 13 and 15 (for amorphous silicon, a thin layer of 5000 Å was deposited, causing contact holes to exhibit double ringlike shapes, which did not change the ellipticity of the contact hole we were investigating). The HARC etch conditions were the same as those in Fig. 2. As shown, both samples experienced decreased ellipticity, i.e., the contact hole shapes were more distorted, with increasing aspect ratio. However, the amorphous carbon had lower ellipticity, and thus more distortion, compared to the amorphous silicon. When the same HARC etch conditions were used, the thickness and characteristics of the polymer layer deposited on the sidewall of the contact hole may not be significantly different for the two mask materials. This is because they are more related to the reactive C-F based species coming from the plasma, while the remaining shapes of the masks can be changed due to the differences in the etch selectivity for the same etch conditions. Therefore, the improved ellipticity of the contact holes by using amorphous silicon versus amorphous carbon may be more related to the change in mask shapes during etching rather than the thickness of the polymer layer on the sidewall of the contact.

In fact, for the same mask material, the change of the mask height itself can affect the ellipticity of the contact for the same etch depth. If the mask height is increased, the

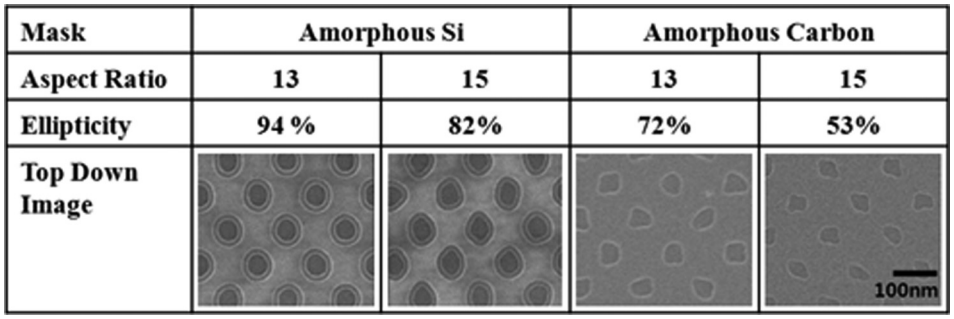

FIG. 4. Effect of mask materials on the contact hole distortion during HARC etching. As the mask materials, an amorphous silicon layer and amorphous carbon layer were used. The HARC etch conditions were the same as those in Fig. 2.

Mask	Amorphous Si		
Mask Height	4 kÅ	5 kÅ	6 kÅ
A/R w/o mask	14.0		
A/R with Mask	18.8	20	21.3
Ellipticity	71 %	80 %	74%
Top Down Image	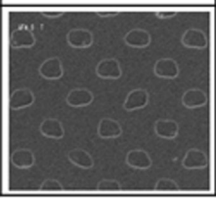	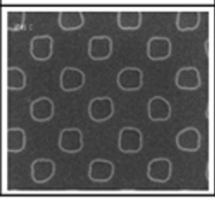	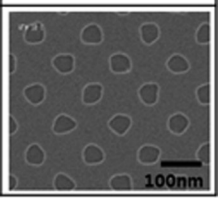

FIG. 5. Effect of mask thickness on the contact hole distortion for a fixed HARC etch depth. The HARC etch conditions were the same as those in Fig. 2.

ellipticity is degraded due to the increase in aspect ratio, as shown in Fig. 2. However, if the mask height is too shallow, even though the aspect ratio is decreased, the contact hole shape is again degraded due to the transfer of the locally eroded mask shape to the contact hole. Therefore, an optimized mask thickness is helpful in improving the ellipticity of the contact. Figure 5 shows the effect of mask height on the contact hole distortion at a fixed HARC etch depth. The HARC etch conditions were the same as those in Fig. 2. As shown in the figure, when the aspect ratio is decreased from 21.3 to 20 (when the mask height was not considered, the aspect ratio was 14) by decreasing the amorphous silicon layer thickness from 6 to 5 kÅ, the ellipticity was improved from 74% to 80%. Thus, we conclude that a thinner mask improves ellipticity, due to the decreased aspect ratio. However, when the mask height was further decreased to 4 kÅ, the ellipticity of the contact was again degraded to 71%. The degrading of the contact hole shape by further decreasing the mask height to 4 kÅ is believed to be related to the transfer of the eroded mask shape to the contact hole shape caused by local degradation of the thin mask layer.

Figure 6 shows (a) a cross-sectional SEM image and (b) a top–down SEM image of a locally degraded amorphous silicon mask layer (4 kÅ mask height) obtained during HARC etching. Due to the thinness of the mask, the mask layer was locally degraded during etching, as shown in Fig. 6(a), and

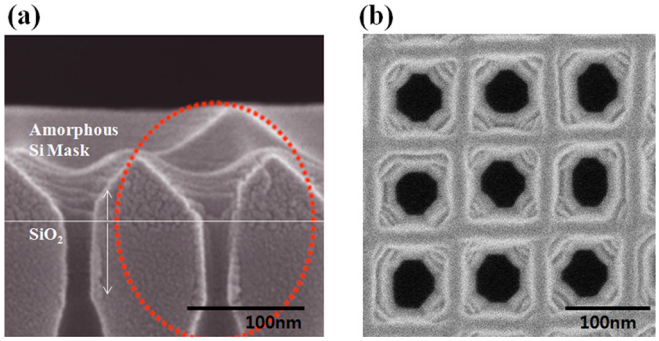

FIG. 6. (Color online) (a) Cross-sectional view of a locally degraded mask layer and (b) top–down view of the mask.

the degraded mask shape appears to have transferred to the contact hole during the HARC etching and resulted in the contact hole distortion as shown in Fig. 6(b). Therefore, the mask height is believed to affect the ellipticity of the contact hole during HARC etching and needs to be optimized to obtain the least contact hole distortion.

As mentioned above, the thickness and characteristics of the polymer layer deposited on the sidewall of the contact hole can be more affected by the reactive C-F based species coming from the plasma during HARC etching. In general, for HARC etching, a multistep HARC etching method composed of a main etch step and an overetch step is used and, during the overetch step, a C-F based polymer-rich gas mixture is used to improve the etch selectivity with the exposed underlayer. Therefore, in this experiment, the etch gas composition was varied during the overetch step and the effect of overetch gas chemistry on the contact hole distortion was investigated. Figure 7 shows SEM images of the contact holes after etching with different overetch gas mixtures. SEM images were taken at the aspect ratio of 20 and with amorphous silicon as the etch mask (mask was not locally degraded during etching). For the main etch gas chemistry, $C_4F_8/O_2/Ar$ was used, while $C_4F_8/O_2/Ar$ and/or $C_4F_6/O_2/Ar$ were used for the overetch steps. C_4F_6-based gas tends to generate more high-molecular weight radicals that act as polymer-rich precursors in the plasma compared to C_4F_8-based gas, due to a higher C/F ratio. Therefore, a thicker polymer layer is expected on the mask and the top sidewall of the contact for the C_4F_6-based gas during the overetching. As shown in Fig. 7, the use of C_4F_6-based gas for the overetch step led to more degraded ellipticity compared to C_4F_8-based gas after the overetching. Increasing the overetching portion using C_4F_6-based gas degraded the ellipticity further due to the thicker polymer deposition during the etching. Therefore, the contact distortion appears to also be affected by the most polymerizing etch step of the HARC etching process.

From our results, it can be concluded that the contact distortion is not directly affected by the local polymer thickness deposited on the sidewall of the contact hole. Rather, it is more affected by the polymer thickness and the nonuniform

Main Etch	C_4F_8			
Over Etch 1	C_4F_6	C_4F_6	C_4F_8	C_4F_8
Over Etch 2		C_4F_8	C_4F_6	
Ellipticity	80 %	81%	82%	86%
Top Down Image	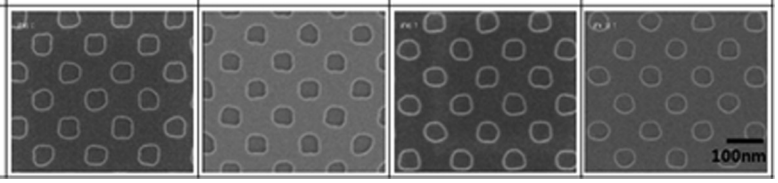			

FIG. 7. Comparison of contact distortion for the different C-F based etching chemistries during the overetching of a multistep HARC etching. The aspect ratio of the contact was 20 and amorphous silicon was used as the etch mask. During the main HARC etching, $C_4F_8/O_2/Ar$ was used while $C_4F_8/O_2/Ar$ and/or $C_4F_6/O_2/Ar$ were used for the overetch step.

polymer layer deposited on the top sidewall of the contact during the polymerizing etch step. Also, if the thickness of the mask layer is not thick enough, the contact distortion can be affected by the local mask degradation if the degraded mask pattern is transferred to the contact. In fact, the nonuniform and thick polymer deposited on the sidewall of the contact can be alleviated by using a less polymerizing C-F based gas such as C_4F_8 for both the main etch step and the overetch step, as shown in Fig. 7. However, the use of less polymerizing C-F based gas, especially during the overetch step, can not satisfy the required etch selectivity over the underlayer exposed after the main etch step and, therefore, is not feasible for actual HARC etch processing.

A polymer removal step was thus inserted in the overetch step to etch the HARC selectively over the underlayer by using a polymer-rich etch gas chemistry, while *in-situ* removing excessive polymer deposited on the top sidewall of the contact hole. Figure 8 shows the SEM images of the contact bottom area etched with/without a polymer removal step during overetching steps of HARC etching from Fig. 7 (the aspect ratio was 20:1). C_4F_8-based gas was used for the main etch step and C_4F_6-based gas was used for the overetch steps. As shown in Fig. 8, when a polymer removal step was added after the partial overetching (over etch 1), by removing the nonuniform polymer deposited on the top sidewall of the contact, the contact hole size was increased. After etching the HARC using C_4F_6-based gas further (over etch 2), a contact ellipticity of 87% was measured, which is about 7% higher than that etched without the polymer removal step. Just by adding a polymer removal step to the same multistep HARC etching process, an improvement in the contact distortion was observed. In addition, this optimized multistep HARC process was applied to the capacitor patterning process of a dynamic random access memory device fabrication and the contact resistances were measured for a wafer scale. The result showed that, by simply adding a polymer residue removal step during the overetching, an improvement in contact resistance of about 12% could be obtained by improving the contact distortion, and, therefore, by increasing the contact area (not shown).

Main Etch	C_4F_8			
Over Etch 1	C_4F_6	C_4F_6	C_4F_6	C_4F_6
Polymer Removal	Skip	O	O	
Over Etch 2		Skip	C_4F_6	
Top Down Polymer Image	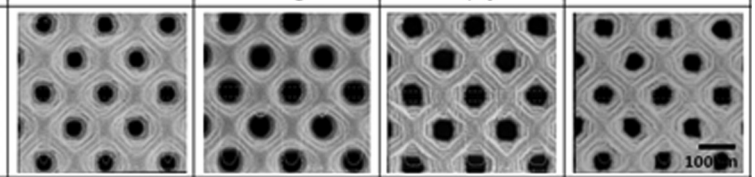			
Contact Bottom Distortion Image	-	-	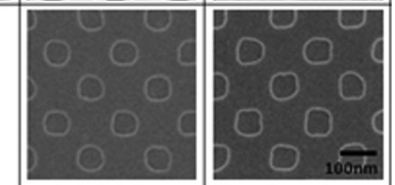	
Ellipticity	-	-	87%	80%

FIG. 8. Comparison of bottom contact distortion with/without a polymer removal step during overetching steps of HARC etching. C_4F_8-based gas was used for the main etch step and C_4F_6-based gas was used for the overetch steps. The main etch conditions and other overetch conditions are the same as those in Fig. 7.

IV. CONCLUSIONS

HARC etching is becoming a crucial process as semiconductor devices are decreasing to subnanometer scale. In this study, the major factors affecting contact distortion during HARC etching have been investigated by varying etch parameters such as mask material, mask thickness, and etch chemistry. The results showed that the contact distortion is affected by the polymer thickness and nonuniform polymer layer deposited on the top sidewall of the contact during the polymerizing etch step of HARC etching. Also, the contact distortion can be affected by the local mask degradation. If the mask layer is not thick enough, the degraded mask pattern is transferred to the contact. By adding an *in-situ* polymer removal step during the overetch step of a multistep HARC etch process, an improvement in contact distortion of about 7% could be obtained without changing other conditions. It is believed that the technique suggested in this study can be applied further to processing of next-generation devices requiring higher aspect ratio contacts.

ACKNOWLEDGMENTS

This research was supported by the Nano-Material Technology Development Program through the National Research Foundation of Korea (NRF) funded by the Ministry of Education, Science, and Technology (No. 2012M3A7B4035323).

[1]See www.itrs.org for International Technology Roadmap for Semiconductor (2012).
[2]K. Endo, S. I. Ouchi, Y. Ishikawa, L. Yongxun, T. Matsukawa, K. Sakamoto, J. Tsukada, H. Yamauchi, and M. Masahara, IEEE Electron Device Lett. **31**, 546 (2010).
[3]K. Romero, R. Stephan, G. Grasshoff, M. Ruelke, K. Huy, J. Klais, S. Gowan, S. Bell, and M. Wright, IEEE Trans. Semiconduct. Manuf. **18**, 539 (2005).
[4]C. Y. Ho, H. J. Kin, H. R. Chien, and C. Lien, Thin Slid Films **518**, 6076 (2010).
[5]S. W. Cho, C. K. Kim, J. K. Lee, S. H. Moon, and H. Y. Chae, J. Vac. Sci. Technol., A **30**, 051301 (2012).
[6]S. Samukawa and T. Mukai, J. Vac. Sci. Technol., B **18**, 166 (2000).
[7]A. C. Westerheim, A. H. Labun, J. H. Dubash, J. C. Arnold, H. H. Sawin, and V. Y. Wang, J. Vac. Sci. Technol., A **13**, 853 (1995).
[8]D. Fuard, O. Joubert, L. Vallier, M. Assous, P. Blanc, and R. Blanc, J. Vac. Sci. Technol., B **19**, 2223 (2001).
[9]N. Fujiwara, S. Ogino, T. Maruyama, and M. Yoneda, Plasma Surf. Sci. Technol. **5**, 126 (1996).
[10]S. Banna *et al.*, IEEE Trans. Plasma Sci. **37**, 1730 (2009).
[11]T. Shimmura, S. Soda, S. Samukawa, M. Koyanagi, and K. Hane, J. Vac. Sci. Technol., B **20**, 2346 (2002).
[12]D. S. Kim, E. A. Hudson, D. Cooperberg, E. Edelberg, and M. Srinivasan, Thin Solid Films **515**, 4874 (2007).